Faraday Discussions

Accepted Manuscript

This manuscript will be presented and discussed at a forthcoming Faraday Discussion meeting. All delegates can contribute to the discussion which will be included in the final volume.

Register now to attend! Full details of all upcoming meetings: http://rsc.li/fd-upcoming-meetings

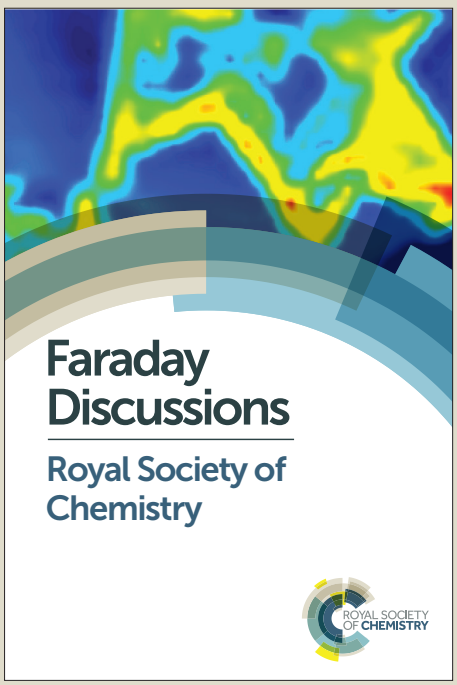

This is an *Accepted Manuscript*, which has been through the Royal Society of Chemistry peer review process and has been accepted for publication.

Accepted Manuscripts are published online shortly after acceptance, before technical editing, formatting and proof reading. Using this free service, authors can make their results available to the community, in citable form, before we publish the edited article. We will replace this *Accepted Manuscript* with the edited and formatted *Advance Article* as soon as it is available.

You can find more information about *Accepted Manuscripts* in the Information for Authors.

Please note that technical editing may introduce minor changes to the text and/or graphics, which may alter content. The journal's standard Terms & Conditions and the Ethical guidelines still apply. In no event shall the Royal Society of Chemistry be held responsible for any errors or omissions in this *Accepted Manuscript* or any consequences arising from the use of any information it contains.

ROYAL SOCIETY OF CHEMISTRY

www.rsc.org/faraday_d

CREATED USING THE RSC LaTeX PCCP ARTICLE TEMPLATE – SEE www.rsc.org/electronicfiles FOR DETAILS
PAPER www. rsc.org/faraday_d | Faraday Discussions

A design equation for low dosage additives that accelerate nucleation

Geoffrey G. Poon,[a] Stefan Seritan,[a] and Baron Peters*[ab]

Received Xth XXXXXXXXXX 20XX, Accepted Xth XXXXXXXXX 20XX
First published on the web Xth XXXXXXXXXX 200X
DOI: 10.1039/c000000x

Additives are used to control nucleation in many natural and industrial environments. However, the mechanisms by which additives inhibit or accelerate solute precipitate nucleation are not well understood. We propose an equation that predicts changes in nucleation barriers based on the adsorption properties and concentrations of trace additives. The equation shows that nucleant efficacy depends on the product of an adsorption equilibrium constant and the reduction in interfacial tension. Moreover, the two factors that determine potency of additives are related to each other, suggesting that assays of just one property might facilitate additive design. We test the design equation for a Potts-lattice gas model with surfactant-like additives in addition to solutes and solvents.

1 Introduction

Metastable phases of matter include liquids that can be supercooled without freezing, vapors that can be supercooled without condensing, and solids that can exist as multiple polymorphs. Some metastable phases can survive for long times because the more stable phase cannot form without first surmounting an activation barrier for nucleation. Nucleation is a stochastic process that forms the first growing embryo of the more stable phase. Nucleation and growth from single component systems have been extensively studied, but there has been relatively little theoretical and computational work on solute precipitate nucleation. Even fewer studies have focused on nucleation in the presence of additives.

Additives are important in nucleation and growth in many natural and industrial processes including ice formation,[1–5] pharmaceutical crystallization,[6–8] biomineralization,[9–16] and material synthesis.[17–20] For example, pharmaceutical companies use nucleants, growth promoters, and inhibitors to drive the selective crystallization of the desired polymorph.[21–24] Oil and gas companies invest millions of dollars on inhibitors to prevent methane hydrates from clogging pipelines.[25–27] Others have investigated additives to accelerate gas hydrate formation for gas storage at moderate temperatures and pressures.[28–31] In biology, salts, metabolytes, and proteins prevent the formation of urinary stones[32,33]

[a] *Department of Chemical Engineering, University of California, Santa Barbara, California 93106, USA. E-mail: baronp@engineering.ucsb.edu*
[b] *Department of Chemistry, University of California, Santa Barbara, California 93106, USA.*

Faraday Discussions Accepted Manuscript

and ice in Antarctic fish.[34–36] Therefore, there is substantial scientific and industrial interest in designing additives for controlling nucleation and growth. Additives are currently discovered by trial-and-error experiments rather than focused searches guided by physical models.

Classical nucleation theory (CNT) predicts that nucleation rates are primarily dependent on two competing factors: (1) the bulk chemical potential difference between the stable and metastable phases and (2) the interfacial free energy between the two phases.[37,38] The first factor is the nucleation driving force and is often written in terms of supersaturation (i.e. $\Delta\mu = k_B T \ln S$). The second factor, interfacial free energy, is directly responsible for the nucleation barrier. Although the nucleation barrier can be adjusted by modulating supersaturation, we are primarily interested in additives that selectively bind to the nucleus and lower the interfacial free energy. Surface-active additives can potentially have strong effects on nucleation at trace concentrations.

Most experimental and theoretical research on trace additives focus on crystal growth, not nucleation. For example, Weissbuch and coworkers have experimentally studied "tailor-made" stereospecfic promoters and inhibitors that drive the selective crystallization of polymorphs.[39,40] Ward and coworkers studied molecular inhibitors that bind stereospecifically to growing crystal faces and suppress growth.[33,41] Storr et al.[26] and Anderson et al.[25] used molecular simulations to compare binding energies of hydrate growth inhibitors. All of these works investigate the effect of additives on large crystal surfaces instead of the microscopic clusters present during the nucleation stage.

A few recent theoretical studies investigated the effect of additives on nucleation, but these did not separately consider the interfacial and solubility contributions to the free energy barrier. Anwar et al. used short unbiased molecular simulations of a ternary Leonard Jones (LJ) system (i.e. solute-solvent-additive) to compare nucleation rates for different additive interaction and size parameters.[42] Duff et al. developed an alchemical transformation approach to compare the effects of NaCl on the interfacial free energy of nuclei for two polymorphs of glycine.[43] However, Duff et al. did not compute the effect of salt on the solubility of glycine in solution, a separately important effect of adding salt.

This paper proposes a theoretically-motivated additive design equation that applies to low dosage nucleation promoters that strongly interact with the solution-precipitate interface. The equation is motivated by (1) the barrier's strong dependence on interfacial tension, (2) the drop in interfacial tension with increasing additive interfacial coverage, and (3) the increase in coverage with increasing additive concentration. It predicts a drop in barrier height proportional to trace additive concentration. The proportionality constant is the product of two measurable quantities: an equilibrium constant for adsorption and the reduction in interfacial tension per unit coverage. These two quantities are related to each other, so a method to quickly determine either property for a set of trial additives could help design potent nucleation promoters.

 This journal is © The Royal Society of Chemistry [year]

Faraday Discussions Accepted Manuscript

2 Theory

CNT predicts that the reversible work to grow a nucleus from $n = 1$ building units to a size n is:[37,38,44–47]

$$F(n) = -n\Delta\mu + \gamma a\phi n^{2/3} \tag{1}$$

where the free energy $F(n)$ depends on the chemical potential difference between the metastable and stable phases ($\Delta\mu$), the interfacial tension (γ), the area per adsorption site (a), and a shape factor (ϕ) such that $N_{site} = \phi n^{2/3}$ is the number of adsorption sites on the interface. The qualitative dependence of free energy on cluster size in Equation 1 is supported by many previous simulations.[48–57]

According to Equation 1, the free energy barrier scales with the cube of interfacial tension:

$$F^{\ddagger} = \frac{4}{27}\left[\frac{(\gamma a\phi)^3}{\Delta\mu^2}\right] \tag{2}$$

where $F^{\ddagger}$ is the work required to create a critical nucleus of size $n^{\ddagger} = (2\gamma a\phi/3\Delta\mu)^3$ at which $\partial F/\partial n = 0$. While the free energy barrier is strongly dependent on the driving force, large loadings of additives would generally be required to alter the driving force. By contrast, additives that selectively interact with the interface can lower the interfacial tension and therefore promote nucleation at low concentrations. CNT predicts the change in the free energy barrier due to a change in the interfacial tension when the driving force is held constant is:

$$\frac{F^{\ddagger} - F_0^{\ddagger}}{F_0^{\ddagger}} = \left(\frac{\gamma}{\gamma_0}\right)^3 - 1 \tag{3}$$

where the subscript 0 indicates the reference value with no additives present.

In the simplest case, suppose additive adsorption follows the Langmuir isotherm:

$$\theta = \frac{Kx}{1 + Kx} \tag{4}$$

where θ is the fraction of adsorption sites occupied by additives, K is the Langmuir constant, and x is the additive concentration.[58,59] Langmuir type adsorption assumes localized adsorption onto uniform surface sites and no interaction between adsorbed molecules, which are both reasonable assumptions for dilute adsorbates. In the dilute limit (i.e. $Kx \ll 1$), Equation 4 is simplified to a relationship resembling Henry's law:[58,59]

$$\theta \approx Kx \tag{5}$$

where K is now just the equilibrium constant of adsorption.

The change in interfacial energy upon addition of additives $\gamma - \gamma_0$ can be related to additive coverage on the interface θ as depicted in the thermodynamic cycle of Figure 1:

$$[\gamma(\theta) - \gamma_0]\, a = \theta \Delta F_{ads}^{\circ} \tag{6}$$

where ΔF_{ads}° is the average interfacial free energy change for adsorption at the reference state and θ is the fraction of adsorption sites occupied by an additive. Since $\Delta F_{ads}^{\circ} = -k_B T \ln K$,[58] Equation 6 can be simplified to:

Faraday Discussions Accepted Manuscript

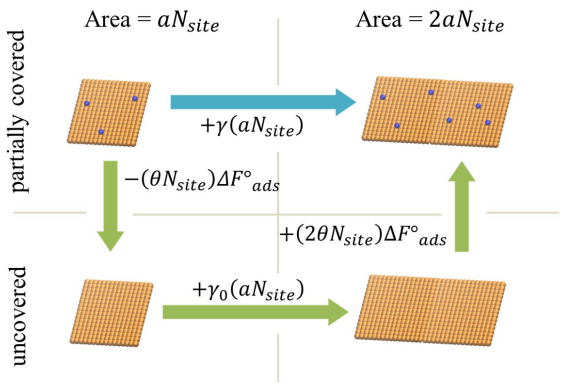

Fig. 1 The reversible work to double the area of a partially covered surface (blue path) is equivalent to the work to (1) remove the additives from the surface, (2) double the surface area, and (3) adsorb the same fraction of additives on the surface (green path).

$$\gamma(\theta) - \gamma_0 = -\frac{K \ln K}{a} x \tag{7}$$

which, in agreement with the Gibbs adsorption isotherm,[58,59] shows that interfacial tension decreases if additives favorably adsorb to the interface. Equation 7 is also consistent with the linear reduction in surface tension for small concentrations of surfactants.[60]

Note, however, that Equations 6 and 7 are only valid in the dilute limit when the adsorbed additives do not interact. The model must break down for sufficiently large θ else negative γ would result. Additionally, Equation 7 ignores the effects of additives that can dissolve into the solid precipitate and additives that preferentially bind at surface defects like kinks, steps, and pits.

For our idealized model in which dilute additives sparingly cover smooth surfaces of the nuclei, Equations 3 and 7 can be combined to obtain:

$$\frac{F^{\ddagger}(x) - F_0^{\ddagger}}{F_0^{\ddagger}} \approx -3\frac{K \ln K}{\beta a \gamma_0} x \tag{8}$$

where $\beta = 1/k_B T$. Equation 8 predicts relative changes in free energy barriers with additive concentration. Instead of the equilibrium adsorption constant K, the change in free energy barrier can equally be written entirely in terms of $\gamma - \gamma_0$. Both forms are potentially useful for screening additives, e.g. by computing adsorption equilibria K or by measuring changes in contact angles $\gamma - \gamma_0$ for trial additives.

Note that nucleation rates depend on free energy barriers as $J = A \exp[-\beta \Delta F^{\ddagger}]$. Assuming that the prefactor is only weakly dependent on additive concentration, Equation 8 further suggests that:

$$\ln\left[J(x)/J_0\right] \approx \frac{3F_0^{\ddagger}}{a\gamma_0}(K \ln K)x \tag{9}$$

where $J(x)$ and J_0 are nucleation rates with and without additives respectively. Using Equation 2, the quantity $3F_0^{\ddagger}/a\gamma_0$ can be written as $\phi(2\gamma_0 a\phi/3\Delta\mu)^2$.

This journal is © The Royal Society of Chemistry [year]

Faraday Discussions Accepted Manuscript

Thus, assuming spherical nuclei and given values for $\Delta\mu$ and K, Equation 9 offers an intriguing new method for extracting the bare interfacial tension (γ_0) from the slope of $\ln[J/J_0]$ as a function of additive concentration (x). Equation 9 also conveniently separates the effect of non-additive properties ($3F_0^{\ddagger}/a\gamma_0$) from additive-specific properties ($K \ln K$) and suggests that the efficacy of nucleation promoters can be compared using ratios of $K \ln K$.

3 Simulation methods

3.1 Ternary Potts lattice gas model

Lattice models enable the investigation of metastable solutions independent of system-specific chemical details.[61,62] They are frequently used to test new rare event algorithms and to provide general insight into nucleation but primarily on single component systems. A number of studies have combined lattice gas simulations with theoretical analyses based on CNT.[62–65] For example, Pan and Chandler studied the transition state ensemble of critical nuclei of an lattice gas model and confirmed that cluster size is a reasonable reaction coordinate for nucleation.[49] Sear used lattice gas models to investigate heterogeneous nucleation in pores of different shapes and sizes.[66–68]

The Potts model is a generalization of the lattice gas model with each Potts orientation representing a particular phase or component[69,70] and has been used to study structural transitions in solids.[71,72] Peters and coworkers developed a binary Potts lattice gas (PLG) model with a lattice gas-like degree of freedom to distinguish between lattice sites occupied by solutes or solvents and a Potts-like degree of freedom to represent the orientation of molecules or lattice vectors at each lattice site.[56,73] The PLG model is a minimal nearest-neighbor model for orientation-specific interactions between solute-solute, solute-solvent, and solvent-solvent pairs. The interaction parameters can be tuned to obtain phase diagrams that resemble those of real binary mixtures. The PLG and closely related models have now been used in studies of phase equilibria, self-assembly, and several nucleation processes.[56,73–78]

The model in this work starts with the PLG and incorporates additives as a third component. Each lattice site is therefore occupied by either a solute, solvent, or additive (labeled species $k = 1$, 2, and 3 respectively) having one of $Q = 24$ possible orientations. For a cubic lattice, $Q = 24$ represents the most asymmetric case,[79] but smaller values of Q can be used to represent more symmetric molecules.[57,80] The PLG Hamiltonian takes solute-solvent interactions as the zero of energy and sums over all nearest neighbor solute-solute, solvent-solvent, and additive-solute interactions. Using the notation $\langle i, j \rangle$ to denote nearest neighbor pairs, the Hamiltonian is:

$$\beta H = \beta H_0 + \beta \Delta H \tag{10}$$

where $\beta\Delta H$ and βH_0 are the additive and additive-free Hamiltonians respectively. The solute-solute and solvent-solvent interactions are those of the standard

Faraday Discussions Accepted Manuscript

PLG model:

$$\beta H_0 = -\sum_{k=1}^{2}\sum_{\langle i,j\rangle}\delta_{m(i),k}\delta_{m(j),k}\left[\beta G_k + \beta A_k \delta_{s(i),s(j)}\right] \tag{11}$$

where $m(i)$ represents the species at lattice site i, $s(i)$ represents the local orientation of the molecule at lattice site i, and βG_k and βA_k are the species-specific and orientation-specific interaction respectively. βG_1 and βG_2 stabilize solute-solute and solvent-solvent pairs respectively and primarily control the solubility of solute in the solvent-rich phase and solvent in the solute-rich phase. Like neighbors with matching orientations are further stabilized by βA_1 and βA_2. For this study, we use the following PLG Hamiltonian parameters: $\beta G_1 = \beta G_2 = \beta A_1 = 1.25$ and $\beta A_2 = 0$. This choice of PLG parameters results in a weakly soluble solute and a relatively pure solute precipitate identical to the binary PLG model shown on Figure 1a of Duff and Peters at $k_B T = 0.8$.[56,79]

The additives mimic amphiphilic molecules through interactions that favor adsorption at the solute precipitate-solution interface. Additive-solvent and additive-additive interactions are equivalent to the zero energy solute-solvent interactions, making the additives sparingly soluble in solution and preventing them from aggregating. Additives interact with solutes only along the direction of their orientation:

$$\beta\Delta H = -\sum_{\langle i,j\rangle}\delta_{m(i),3}\delta_{m(j),1}\delta_{g(i),n(j,i)}\beta A_3 \tag{12}$$

where $n(j,i)$ is the neighbor index of lattice site j with respect to lattice site i which varies from 1 to 6 for a cubic lattice and $g(i)$ indexes the neighbor to which the orientation of the additive at lattice site i points. For a cubic lattice, $g(i) = \mod[Q,6]+1$ (i.e. 1 plus the remainder of $Q/6$) also varies from 1 to 6. Therefore, only additives whose orientation points toward a solute experiences a favorable interaction (see Figure 2). This directional additive-solute interaction

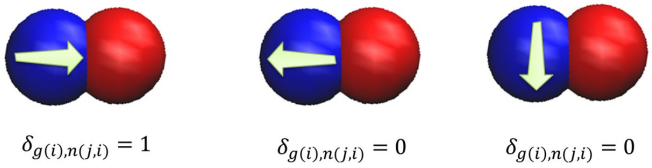

Fig. 2 The additive (blue) only interacts with a neighboring solute if its orientation points toward a solute (red), i.e. $g(i) = n(j,i)$.

mimics the attraction between the head/tail group of surfactants and the interface and prevents the nucleating phase from having many additive inclusions even though their interactions are strong. For this study, we used five different values of βA_3 to investigate the effect of additive binding strength: $\beta A_3 = 2.5$, 2.875, 3.125, 3.375 , and 3.75.

3.2 Simulation details

In a small closed simulation with fixed composition, a solute nucleus depletes the solute from its surroundings and consumes the driving force for its own

 This journal is © The Royal Society of Chemistry [year]

Faraday Discussions Accepted Manuscript

growth.[47,81–84] Because of these finite size effects, solute precipitate nucleation is best simulated in the grand or semigrand (open) ensembles.[47,56,73,85] We use semigrand canonical Monte Carlo (SGMC) (or NT$\{\mu_i - \mu_r\}$ ensemble) simulations[86] to maintain differences in chemical potentials of each species and that of the solvent reference species. Our SGMC moves include (1) local and nonlocal swaps, (2) orientation flips, and (3) semigrand identity changes. The first two move types are accepted or rejected using the standard canonical Metropolis criterion. The acceptance probability for identity changes from species i to j involves an additional fugacity ratio prefactor.[86]

Free energy landscapes along the nucleus size coordinate n are computed as:

$$\beta F(n) = -\ln \frac{\langle N(n)\rangle}{\langle N(1)\rangle} \tag{13}$$

where $\langle N(n)\rangle$ is the average number of nuclei composed of n solute monomers in the simulation box.[47,51,52] The size n of each nucleus is computed by counting contiguously neighboring solutes. However, it is computationally impractical to calculate $F(n)$ using unbiased Boltzman sampling for high barrier processes due to the exponentially vanishing probability of visiting higher free energy states. We overcome this issue with umbrella sampling which imposes a set of artificial biasing potentials to improve sampling of less probable configurations.[87–89] We use windows of width three units along the nucleus size n-coordinate with hard walls at the window edges. Each umbrella window is sampled for at least 500,000 SGMC sweeps to guarantee sufficient sampling.

3.2.1 Compositions of equal driving force. The nucleation free energy barrier depends on both the driving force (or supersaturation) and interfacial free energy. To isolate the effects of the additive on the interfacial free energy, we prepared compositions of equal driving force. The driving force is measured by simulating slab growth in a long elongated cell (in this case a 10x10x80 lattice) which maximizes the volume to surface ratio for a two phase system. The change in free energy for layer-by-layer slab growth is $F_{slab}(n) - F_{slab}(n_0) = -(n - n_0)\Delta\mu$.

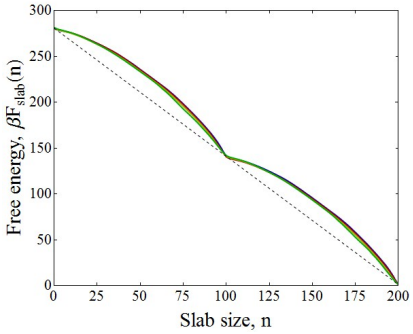

Fig. 3 The free energy landscape of solute slab growth at different fugacity ratios with the same driving force for $\beta A_3 = 3.75$. The driving force $\Delta\mu$ is estimated by the common tangent through troughs (dashed line).

Faraday Discussions Accepted Manuscript

The driving force is therefore:[90]

$$\Delta\mu = -\frac{\partial F_{slab}}{\partial n} \tag{14}$$

The set of compositions of constant driving force can be calculated by the following iterative process:

1. Simulate slab growth using SGMC and calculate the dimensionless driving force with no additive ($\beta\Delta\mu_0$) using Equation 14.

2. Adjust the additive-solvent (f_3/f_2) and solute-solvent (f_1/f_2) fugacity ratio and repeat Step 1 until the driving force is approximately $\beta\Delta\mu_0$.

3. Repeat Step 2 for each solute-solvent-additive composition.

Increasing f_1/f_2 will increase the solute concentration and therefore driving force. Increasing f_3/f_2 will increase the additive concentration and therefore increase coverage, lower interfacial tension, and lower barrier height. The four sets of fugacity ratios we use that have the same driving force are: $f_1/f_2 = 2.25$ and $f_3/f_2 = 0$, $f_1/f_2 = 2.25$ and $f_3/f_2 = 0.01$, $f_1/f_2 = 2.258$ and $f_3/f_2 = 0.03$, and $f_1/f_2 = 2.26$ and $f_3/f_2 = 0.05$. These fugacity ratios are used for each metastable state in all other simulations. The composition of each metastable state is determined using unbiased 500,000 sweep-long SGMC simulations on a 64x64x64 periodic lattice.

3.2.2 Free energy barriers and interfacial tension. We use umbrella sampling to compute the work required to grow a nucleus from size 1 to n on a 32x32x32 periodic lattice.[87–89,91] Since the probability of observing more than one cluster of size $n > 4$ in our simulation box is negligible, $N(n)$ for values of $n > 4$ is approximated by the probability that the largest cluster in the system is of size n.[51,52] CNT fits of the free energy landscape with Equation 1 are used to estimate nucleation barriers and interfacial tension.

3.2.3 Additive adsorption. SGMC simulations are used to estimate the adsorption constant. Simulations are done on a 64x64x64 lattice with a 64x64 solute sheet. The sheet is not allowed to grow, dissolve, or change any of its Potts degrees of freedom. Coverage is estimated by averaging the fraction of lattice sites neighboring the solute sheet that is occupied by an additive[92] from at least 500,000 SGMC sweeps.

4 Results and discussion

Figure 4a shows that the average additive coverage θ for a range of average additive mole fraction x agrees with the predicted Henry's law behavior at low concentrations. We obtain the adsorption constant K by fitting additive coverage θ to Equation 5. Figure 5 shows the free energy $F(n)$ for the four compositions of equal driving force for $\beta A_3 = 3.75$, which is qualitatively similar for other values of βA_3. Interfacial tension $\beta a\gamma\phi$ is obtained by fitting $F(n)$ to Equation 1 for each additive concentration with the constraint that the driving force at each additive concentration is the same. The proportional relationships in Figures 4a

 This journal is © The Royal Society of Chemistry [year]

Faraday Discussions Accepted Manuscript

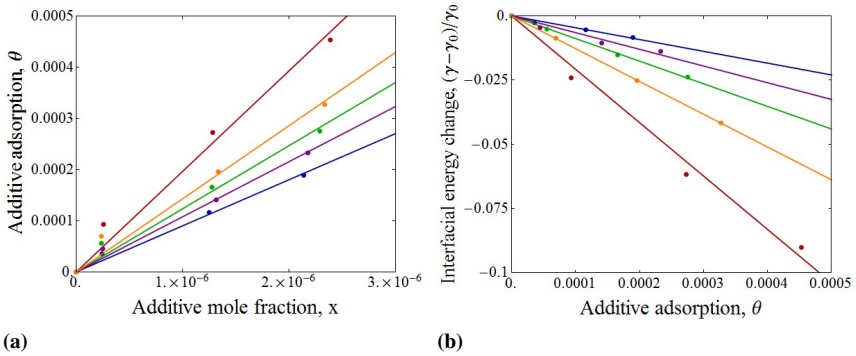

Fig. 4 Proportional relationships between (a) additive coverage θ and additive concentration x and (b) change in interfacial free energy $(\gamma - \gamma_0)/\gamma_0$ and θ. Lines are linear fits constrained to pass through the origin for additive-solute interactions $\beta A_3 = 2.5$ (blue), 2.875 (purple), 3.125 (green), 3.375 (orange), and 3.75 (red).

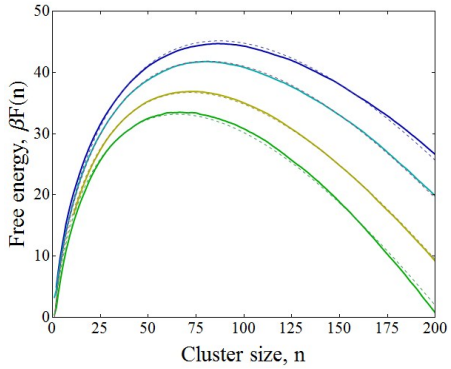

Fig. 5 The reversible work $\beta F(n)$ to create a nucleus of size n at different additive concentrations for $\beta A_3 = 3.75$. The dotted lines are CNT fits with the constraint that the driving force at each additive concentration is the same.

and 4b are consistent with our theoretical prediction that increased adsorption will lower interfacial tension.

For the most weakly binding additives, Figure 6b validates the approximately proportional relationship in Equation 8 between the free energy barrier and $(K \ln K)x$. The discrepancy for additives with large values of K may be due to a breakdown in the infinitely dilute additive assumption due to increased interaction with solute in solution. Even at large values of K, Figure 6b suggests ratios of $K \ln K$ can still be used to predict nucleant efficacy, albeit qualitatively.

5 Concluding remarks

We developed an equation starting from classical nucleation theory to predict the effects of additive binding strength and additive concentration on nucleation barriers. The rate is modulated by a product of the interfacial free energy reduction

Faraday Discussions Accepted Manuscript

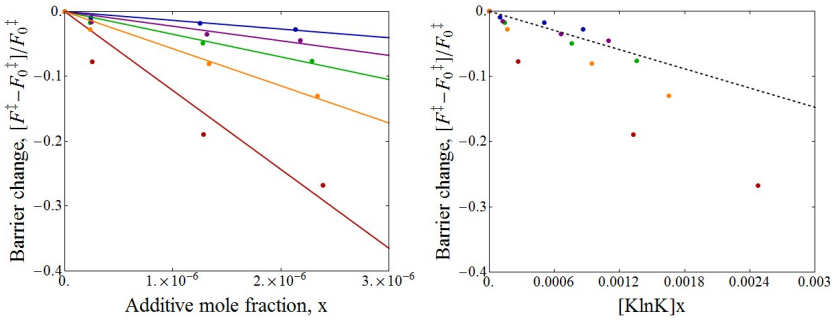

Fig. 6 While (a) changes in free energy barriers are approximately proportional to additive concentration, (b) only additives with small values of βA_3 are consistent with Equation 8. The lines are linear fits that pass through the origin for additive-solute interactions $\beta A_3 = 2.5$ (blue), 2.875 (purple), 3.125 (green), 3.375 (orange), and 3.75 (red). The dashed line is for the combined $\beta A_{13} = 2.5$, 2.875, and 3.125 data.

per unit coverage and the equilibrium constant for additive binding (K). These two quantities are closely related to each other, so it may be possible to screen for potent additives by comparing ratios of $K \ln K$ for trial additives. Promising nucleants can also be screened using contact angle measurements with and without trial additives. Trace additives with higher values of $K \ln K$ are more effective at reducing surface tension, lowering the free energy barrier, and accelerating nucleation. Simulations on a ternary Potts lattice gas model confirm that the potency of a trace additive for barrier reduction increases with $K \ln K$. Further investigations are needed to test the validity of these results for molecular additives, solutes, and solvents.

Acknowledgments

G.G.P acknowledges the National Science Foundation (NSF) for support through the Graduate Research Fellowship under DGE 1144085 and through CBE-1125235. S.S. acknowledges the Summer Undergraduate Research Fellowship (SURF) at the University of California, Santa Barbara for support. B.P. acknowledges the NSF Career Award 955502 for support. We thank Valeria Molinero and Sean Cray for many helpful discussions.

References

1 A. Hudait and V. Molinero, *J. Am. Chem. Soc.*, 2014, **136**, 8081–8093.
2 G. Bullock and V. Molinero, *Faraday Discuss.*, 2013, **167**, 371–388.
3 C. Budke, A. Dreyer, J. Jaeger, K. Gimpel, T. Berkemeier, A. S. Bonin, L. Nagel, C. Plattner, A. L. DeVries, N. Sewald and T. Koop, *Cryst. Growth Des.*, 2014, **14**, 4285–4294.
4 P. A. Alpert, J. Y. Aller and D. A. Knopf, *Atmos. Chem. Phys.*, 2011, **11**, 5539–5555.
5 T. Koop and B. Zobrist, *Phys. Chem. Chem. Phys.*, 2009, **11**, 10839–10850.
6 R. J. Davey, N. Blagden, G. D. Potts and R. Docherty, *J. Am. Chem. Soc.*, 1997, **119**, 1767–1772.
7 N. Blagden and R. J. Davey, *Cryst. Growth Des.*, 2003, **3**, 873–885.
8 A. Llinas and J. M. Goodman, *Drug Discovery Today*, 2008, **13**, 198–210.

 This journal is © The Royal Society of Chemistry [year]

Faraday Discussions Accepted Manuscript

9 V. Pipich, M. Balz, S. E. Wolf, W. Tremel and D. Schwahn, *J. Am. Chem. Soc.*, 2008, **130**, 6879–6892.
10 Y. Levi, S. Albeck, A. Brack, S. Weiner and L. Addadi, *Chem. Eur. J.*, 1998, **4**, 389–396.
11 M. F. Butler, N. Glaser, A. C. Weaver, M. Kirkland and M. Heppenstall-Butler, *Cryst. Growth Des.*, 2006, **6**, 781–794.
12 F. C. Meldrum and H. Coelfen, *Chem. Rev.*, 2008, **108**, 4332–4432.
13 K. Naka and Y. Chujo, *Chem. Mater.*, 2001, **13**, 3245–3259.
14 S. Elhadj, J. J. De Yoreo, J. R. Hoyer and P. M. Dove, *Proc. Natl. Acad. Sci. U. S. A.*, 2006, **103**, 19237–19242.
15 D. Gebauer, H. Coelfen, A. Verch and M. Antonietti, *Advanced Materials*, 2009, **21**, 435–439.
16 D. C. Popescu, M. M. J. Smulders, B. P. Pichon, N. Chebotareva, S.-Y. Kwak, O. L. J. van Asselen, R. P. Sijbesma, E. DiMasi and N. A. J. M. Sommerdijk, *J. Am. Chem. Soc.*, 2007, **129**, 14058–14067.
17 C. Brinker and G. Scherer, *Sol-gel Science: The Physics and Chemistry of Sol-gel Processing*, Academic Press, 1990.
18 R. F. Lobo, S. I. Zones and M. E. Davis, *J. Inclusion Phenom. Mol. Recognit. Chem.*, 1995, **21**, 47–78.
19 Q. S. Huo, D. I. Margolese and G. D. Stucky, *Chem. Mater.*, 1996, **8**, 1147–1160.
20 Y. Kubota, M. M. Helmkamp, S. I. Zones and M. E. Davis, *Microporous Materials*, 1996, **6**, 213–229.
21 O. Galkin and P. G. Vekilov, *Proc. Natl. Acad. Sci. U. S. A.*, 2000, **97**, 6277–6281.
22 P. G. Vekilov, *Cryst. Growth Des.*, 2010, **10**, 5007–5019.
23 V. Y. Torbeev, E. Shavit, I. Weissbuch, L. Leiserowitz and M. Lahav, *Cryst. Growth Des.*, 2005, **5**, 2190–2196.
24 R. P. Sear, *J. Chem. Phys.*, 2001, **115**, 575–579.
25 B. J. Anderson, J. W. Tester, G. P. Borghi and B. L. Trout, *J. Am. Chem. Soc.*, 2005, **127**, 17852–17862.
26 M. T. Storr, P. C. Taylor, J. P. Monfort and P. M. Rodger, *J. Am. Chem. Soc.*, 2004, **126**, 1569–1576.
27 A. K. Sum, C. A. Koh and E. D. Sloan, *Ind. Eng. Chem. Res.*, 2009, **48**, 7457–7465.
28 J. S. Zhang, S. Lee and J. W. Lee, *Ind. Eng. Chem. Res.*, 2007, **46**, 6353–6359.
29 J. S. Zhang, C. Lo, P. Somasundaran, S. Lu, A. Couzis and J. W. Lee, *J. Phys. Chem. C*, 2008, **112**, 12381–12385.
30 A. Fazlali, S.-A. Kazemi, M. Keshavarz-Moraveji and A. H. Mohammadi, *Energy Technology*, 2013, **1**, 471–477.
31 S.-Q. Hao, S. Kim, Y. Qin and X.-H. Fu, *Environ. Chem. Lett.*, 2014, **12**, 341–346.
32 H. X. Yuan and J. M. Ouyang, *Progress in Chemistry*, 2006, **18**, 573–578.
33 J. D. Rimer, Z. An, Z. Zhu, M. H. Lee, D. S. Goldfarb, J. A. Wesson and M. D. Ward, *Science*, 2010, **330**, 337–341.
34 A. L. Devries, *Science*, 1971, **172**, 1152–&.
35 J. G. Duman, *Annu. Rev. Physiol.*, 2001, **63**, 327–357.
36 F. Sicheri and D. S. C. Yang, *Nature*, 1995, **375**, 427–431.
37 D. Kashchiev and G. M. van Rosmalen, *Cryst. Res. Technol.*, 2003, **38**, 555–574.
38 D. Kashchiev, *Nucleation: Basic Theory With Applications*, Butterworth-Heinemann, Oxford, 2000.
39 I. Weissbuch, M. Lahav and L. Leiserowitz, *Cryst. Growth Des.*, 2003, **3**, 125–150.
40 I. Weissbuch, V. Y. Torbeev, L. Leiserowitz and M. Lahav, *Angew. Chem. Int. Ed.*, 2005, **44**, 3226–3229.
41 L. N. Poloni and M. D. Ward, *Chem. Mater.*, 2014, **26**, 477–495.
42 J. Anwar, P. K. Boateng, R. Tamaki and S. Odedra, *Angew. Chem. Int. Ed.*, 2009, **48**, 1596–1600.
43 N. Duff, Y. R. Dahal, J. D. Schmit and B. Peters, *J. Chem. Phys.*, 2014, **140**, 014501.
44 R. Becker and W. Doring, *Annalen der Physik*, 1935, **24**, 719–752.
45 M. Volmer and A. Weber, *Z. Phys. Chem.*, 1926, **119**, 277–301.
46 J. Frenkel, *Kinetic Theory of Liquids*, Dover, 1955.
47 V. Agarwal and B. Peters, *Precipitate Nucleation: A Review of Theory and Simulation Advances*, John Wiley & Sons, New Jersey, USA, 2014, vol. 155.

Faraday Discussions Accepted Manuscript

48 S. Auer and D. Frenkel, *Nature*, 2001, **409**, 1020–1023.
49 A. C. Pan and D. Chandler, *J. Phys. Chem. B*, 2004, **108**, 19681–19686.
50 S. Punnathanam and P. A. Monson, *J. Chem. Phys.*, 2006, **125**, 024508.
51 L. Maibaum, *Phys. Rev. Lett.*, 2008, **101**, 019601.
52 L. Maibaum, *Phys. Rev. Lett.*, 2008, **101**, 256102.
53 S. L. Meadley and F. A. Escobedo, *J. Chem. Phys.*, 2012, **137**, 074109.
54 I. Saika-Voivod, P. H. Poole and R. K. Bowles, *J. Chem. Phys.*, 2006, **124**, 224709.
55 E. Sanz, C. Vega, J. R. Espinosa, R. Caballero-Bernal, J. L. F. Abascal and C. Valeriani, *J. Am. Chem. Soc.*, 2013, **135**, 15008–15017.
56 N. Duff and B. Peters, *J. Chem. Phys.*, 2009, **131**, 184101.
57 B. C. Knott, N. Duff, M. F. Doherty and B. Peters, *J. Chem. Phys.*, 2009, **131**, 224112.
58 J. Kipling, *Adsorption from solutions of non-electrolytes*, Academic Press, 1965.
59 D. Ruthven, *Principles of Adsorption and Adsorption Processes*, Wiley, 1984.
60 S. Safran, *Statistical Thermodynamics of Surfaces, Interfaces, and Membranes*, Addison-Wesley Pub., 1994.
61 K. Binder and H. Muller-Krumbhaar, *Phys. Rev. B*, 1974, **9**, 2328–2353.
62 D. Stauffer, A. Coniglio and D. W. Heermann, *Phys. Rev. Lett.*, 1982, **49**, 1299–1302.
63 J. Schmelzer and D. P. Landau, *International Journal of Modern Physics C*, 2001, **12**, 345–359.
64 V. A. Shneidman, K. A. Jackson and K. M. Beatty, *J. Chem. Phys.*, 1999, **111**, 6932–6941.
65 F. Schmitz, P. Virnau and K. Binder, *Phys. Rev. E*, 2013, **87**, 053302.
66 R. P. Sear, *J. Phys. Chem. B*, 2006, **110**, 4985–4989.
67 R. P. Sear, *J. Phys.: Condens. Matter*, 2012, **24**, 052205.
68 A. J. Page and R. P. Sear, *Phys. Rev. Lett.*, 2006, **97**, 065701.
69 F. Y. Wu, *J. Phys. A: Math. Gen.*, 1981, **14**, L39–L44.
70 F. Y. Wu, *Reviews of Modern Physics*, 1982, **54**, 235–268.
71 R. Devanathan, L. Van Brutzel, A. Chartier, C. Gueneau, A. E. Mattsson, V. Tikare, T. Bartel, T. Besmann, M. Stan and P. Van Uffelen, *Energy & Environmental Science*, 2010, **3**, 1406–1426.
72 V. Tikare, E. A. Holm, D. Fan and L. Q. Chen, *Acta Mater.*, 1998, **47**, 363–371.
73 V. Agarwal and B. Peters, *J. Chem. Phys.*, 2014, **140**, 084111.
74 D. Bellucci, V. Cannillo and A. Sola, *Ceram. Int.*, 2010, **36**, 1983–1988.
75 L. O. Hedges and S. Whitelam, *Soft Matter*, 2013, **9**, 9763–9766.
76 J. Grant, R. L. Jack and S. Whitelam, *J. Chem. Phys.*, 2011, **135**, 214505.
77 W. M. Jacobs, D. W. Oxtoby and D. Frenkel, *J. Chem. Phys.*, 2014, **140**, 204109.
78 T. K. Haxton and S. Whitelam, *Soft Matter*, 2013, **9**, 6851–6861.
79 N. Duff and B. Peters, *J. Chem. Phys.*, 2010, **132**, 129901.
80 B. C. Knott, M. F. Doherty and B. Peters, *J. Chem. Phys.*, 2011, **134**, 154501.
81 D. Reguera, R. K. Bowles, Y. Djikaev and H. Reiss, *J. Chem. Phys.*, 2003, **118**, 340–353.
82 R. Grossier and S. Veesler, *Cryst. Growth Des.*, 2009, **9**, 1917–1922.
83 J. Wedekind, D. Reguera and R. Strey, *J. Chem. Phys.*, 2006, **125**, 214505.
84 A. S. Abyzov and J. W. P. Schmelzer, *J. Non-Cryst. Solids*, 2014, **384**, 8–14.
85 R. Ni, F. Smallenburg, L. Filion and M. Dijkstra, *Mol. Phys.*, 2011, **109**, 1213–27.
86 D. A. Kofke and E. D. Glandt, *Mol. Phys.*, 1988, **64**, 1105–1131.
87 G. M. Torrie and J. P. Valleau, *J. Comput. Phys.*, 1977, **23**, 187–199.
88 S. Kumar, D. Bouzida, R. H. Swendsen, P. A. Kollman and J. M. Rosenberg, *J. Comput. Chem.*, 1992, **13**, 1011–1021.
89 S. Auer and D. Frenkel, *Annu. Rev. Phys. Chem.*, 2004, **55**, 333–361.
90 M. Salvalaglio, T. Vetter, M. Mazzotti and M. Parrinello, *Angew. Chem. Int. Ed.*, 2013, **52**, 13369–13372.
91 B. Roux, *Comput. Phys. Commun.*, 1995, **91**, 275–282.
92 P. Rinaldi, F. Bulnes, A. J. Ramirez-Pastor and G. Zgrablich, *Surf. Sci.*, 2008, **602**, 1783–1794.

Faraday Discussions Accepted Manuscript

 This journal is © The Royal Society of Chemistry [year]